

# Flat-band solutions in $D$ -dimensional decorated diamond and pyrochlore lattices: Reduction to molecular problem

Tomonari Mizoguchi,<sup>1</sup> Hosho Katsura,<sup>2,3,4</sup> Isao Maruyama,<sup>5</sup> and Yasuhiro Hatsugai<sup>1</sup>

<sup>1</sup>*Department of Physics, University of Tsukuba, Tsukuba, Ibaraki 305-8571, Japan\**

<sup>2</sup>*Department of Physics, University of Tokyo, Hongo, Bunkyo-ku, Tokyo 113-0033, Japan*

<sup>3</sup>*Institute for Physics of Intelligence, The University of Tokyo, 7-3-1 Hongo, Bunkyo-ku, Tokyo 113-0033, Japan*

<sup>4</sup>*Trans-scale Quantum Science Institute, University of Tokyo, Bunkyo-ku, Tokyo 113-0033, Japan*

<sup>5</sup>*Department of Information and Systems Engineering, Fukuoka Institute of Technology, Fukuoka 811-0295, Japan*

Flat-band models have been of particular interest from both fundamental aspects and realization in materials. Beyond the canonical examples such as Lieb lattices and line graphs, a variety of tight-binding models are found to possess flat bands. However, the analytical treatment of dispersion relations is limited, especially when there are multiple flat bands with different energies. In this paper, we present how to determine flat-band energies and wave functions in tight-binding models on decorated diamond and pyrochlore lattices in generic dimensions  $D \geq 2$ . For two and three dimensions, such lattice structures are relevant to various organic and inorganic materials, and thus our method will be useful to analyze the band structures of these materials.

## I. INTRODUCTION

Singular dispersions in band structures are the source of a variety of interesting phenomena in solid-state physics. One of the representative examples is a linear dispersion around the band crossing point, or the Dirac/Weyl point [1–3], which gives rise to various intriguing transport [4–6] and magnetic [7–10] phenomena. As such, Dirac/Weyl fermions in solids have been intensively pursued [1–3, 11–13]. Another example of singular dispersion is a flat band, which is a completely dispersionless band in the entire Brillouin zone. Studies of such band structure have been developed in various aspects, such as ferromagnetism [14–20], superconductivity [21–25], topological phenomena [26–42], and localization phenomena [43–48].

So far, various tight-binding models with flat bands have been explored [14, 49–58], and many insights on the model construction have been accumulated. It was also found that some flat-band models have large sublattice degrees of freedom, resulting in multiple flat bands with different energies [59–62]. In such models, it is not easy to obtain analytic expressions of dispersion relations since the Hamiltonians in momentum space are large matrices.

In this paper, we elucidate how to determine the flat-band energies analytically in a class of tight-binding models which can be obtained by decorating the bonds of a honeycomb lattice (in two dimensions), and a diamond lattice (in three dimensions), and their higher-dimensional analogs,  $D \geq 4$ ; see Fig. 1 for the schematic figure of the two-dimensional model. Such lattice structures are of interest because they are known to be realized in various organic-based materials, such as graphene superstructures [63, 64],  $\alpha$ -graphyne [65–68], and metal-

organic frameworks (MOFs) [68–71], as well as some inorganic materials [72, 73]. Recently, they were also discussed in the context of the square-root topological phases [74, 75]. We therefore expect that the determination of the flat-band energies is useful for band structure analysis and material design for these materials.

The key idea is to divide the Hamiltonian into two parts, which we term “linkers” and “linkages”. Importantly, the linkers and the linkages are not independent of each other since they share sites. Nevertheless, the flat-band energies can be obtained by solving the linkage Hamiltonian, and the corresponding wave function can be found such that the compatibility relations are respected on the shared sites. The momentum-independence of the eigenenergies originate from the fact that the linkage Hamiltonian can be regarded as that for an isolated “molecule” [76]. We find that the flat-band wave function

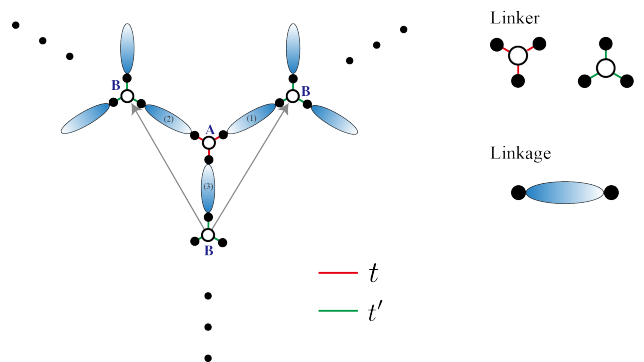


FIG. 1. A schematic of generic decorated diamond lattices. For clarity, we draw the case with  $D = 2$ . White dots stand for the vertices of the original diamond lattice, and gray arrows stand for the lattice vectors. Blue ellipses and black dots denote decorated parts. The schematics of linkers and linkages are also depicted. Note that the black dots belong to both linkers and linkages.

\* mizoguchi@rhodia.ph.tsukuba.ac.jp

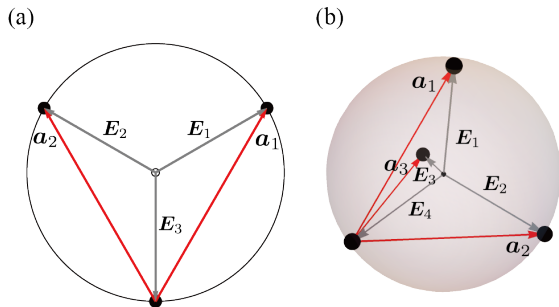


FIG. 2. Schematics of  $\mathbf{a}_j$  and  $\mathbf{E}_j$  of Eq. (1) for (a) two and (b) three dimensions.

of the  $D$ -dimensional decorated diamond lattice is given by the product of the wave function of the linkage and the flat-band wave function of  $D$ -dimensional pyrochlore lattice. We also shed light on another interesting band structure often seen in this class of lattices, namely, a multiple band touching at  $\Gamma$  point which occurs at specific choices of parameters.

The analog of the method described in this paper was previously applied to two-dimensional decorated kagome lattice [62], relevant to covalent organic frameworks (COFs) [60] as well as the cyclicgraphdiyne [77], where carbon atoms having different kinds of  $sp$  hybrid orbitals coexist and form a crystal. Here we emphasize that this method yields not only the energies of the flat bands but also their wave functions, which was not addressed in the previous work. Therefore, for completeness, we also explain the method for obtaining flat-band energies and eigenstates for the  $D$ -dimensional decorated pyrochlore lattice.

In the following discussions in the main text, we impose several assumptions (see Sec. II A) in order to retain the relevance to real materials. However, from a theoretical point of view, some of the assumptions can be relaxed. Such generalizations are described in Sec. V as well as Appendix A.

## II. FLAT-BAND SOLUTIONS FOR $D$ -DIMENSIONAL DECORATED DIAMOND LATTICES

In this section, we first describe the decorated diamond model, which is the main focus of this paper. We then explain how the flat-band energies and wave functions can be determined. The key idea is to employ a tech-

nique of mathematical physics by which we can reduce the eigenvalue problem of the Bloch Hamiltonian with a relatively large size to that of the small molecule.

### A. Model

Consider a diamond lattice in  $D$  dimensions with  $D \geq 2$  [51, 81–83]. The lattice vectors are given as [51]

$$\mathbf{a}_j = \mathbf{E}_j - \mathbf{E}_{D+1}, \quad (1)$$

where  $j = 1, \dots, D$  and the vectors  $\mathbf{E}_1, \dots, \mathbf{E}_{D+1}$  are the vertices of the  $D$ -simplex; see Fig. 2 for the schematics of  $D = 2, 3$ . We set the coordinates of two sublattices of the  $D$ -dimensional diamond lattice (for  $D = 2$ , see the white dots of Fig. 1) as

$$\mathbf{r}_A = \frac{1}{D+1} \sum_{j=1}^D \mathbf{a}_j, \quad (2)$$

and

$$\mathbf{r}_B = \mathbf{0}. \quad (3)$$

Now, let us consider the decorated lattices of  $D$ -dimensional diamonds, shown in Fig. 1. Namely, we decorate the nearest-neighbor (NN) bonds of the diamond lattices, obeying the following rules:

- The sublattices A and B of the original diamond lattice are, respectively, connected to  $D+1$  sites with the same hoppings (red and green bonds in Fig. 1).
- The decorated objects are the same for all the NN bonds of the diamond lattices [see Eq. (7) for details].

For later use, let us clarify some terminologies:

- We call a set of  $D+2$  sites, composed of one site placed on the original diamond lattice and the other  $D+1$  sites connected to that site, a “linker”.
- We call a decorated part on each edge of the diamond lattice a “linkage”. In other words, the linkages are placed on the vertices of the line graph of the diamond lattice.

It is worth noting that the black dots in Fig. 1 belong to both a linker and a linkage.

On this class of lattices, we consider the following Hamiltonian in  $\mathbf{k}$ -space, which is in general written as a  $[(D+1)q+2]$ -dimensional matrix:

$$\mathcal{H}_{\mathbf{k}} = \begin{pmatrix} U_A & t\mathbf{x}_q^T & t\mathbf{x}_q^T & \cdots & t\mathbf{x}_q^T & 0 \\ t\mathbf{x}_q & \mathcal{H}_{\text{linkage}}^{(1)} & \mathcal{O}_q & \cdots & \mathcal{O}_q & t'e^{i\mathbf{k}\cdot\mathbf{a}_1}\mathbf{y}_q \\ t\mathbf{x}_q & \mathcal{O}_q & \mathcal{H}_{\text{linkage}}^{(2)} & \ddots & \vdots & t'e^{i\mathbf{k}\cdot\mathbf{a}_2}\mathbf{y}_q \\ \vdots & \vdots & \ddots & \ddots & \mathcal{O}_q & \vdots \\ t\mathbf{x}_q & \mathcal{O}_q & \cdots & \mathcal{O}_q & \mathcal{H}_{\text{linkage}}^{(D+1)} & t'\mathbf{y}_q \\ 0 & t'e^{-i\mathbf{k}\cdot\mathbf{a}_1}\mathbf{y}_q^T & t'e^{-i\mathbf{k}\cdot\mathbf{a}_2}\mathbf{y}_q^T & \cdots & t'\mathbf{y}_q^T & U_B \end{pmatrix}, \quad (4)$$

where  $\mathbf{x}_q$  and  $\mathbf{y}_q$  are  $q$ -component column vectors defined as  $\mathbf{x}_q := (1, 0, \dots, 0)^T$  and  $\mathbf{y}_q := (0, \dots, 1)^T$ , respectively, and  $\mathcal{O}_q$  stands for the  $q \times q$  zero matrix. The parameters,  $U_A$  and  $U_B$ , are on-site potentials for sublattices A and B, respectively;  $t$  and  $t'$  are, respectively, the transfer integrals assigned on the bonds connecting the decorated part with the sublattices A and B.

For later use, we define two  $(D+1)$ -component row vectors,  $\psi^{(1)\dagger}$  and  $\psi_{\mathbf{k}}^{(2)\dagger}$ , which have the forms:

$$\psi^{(1)\dagger} = (1, 1, \dots, 1), \quad (5a)$$

and

$$\psi_{\mathbf{k}}^{(2)\dagger} = (e^{-i\mathbf{k}\cdot\mathbf{a}_1}, \dots, e^{-i\mathbf{k}\cdot\mathbf{a}_D}, 1), \quad (5b)$$

and the matrix composed of these two vectors [78]:

$$\Psi_{\mathbf{k}}^\dagger = \begin{pmatrix} \psi^{(1)\dagger} \\ \psi_{\mathbf{k}}^{(2)\dagger} \end{pmatrix}. \quad (6)$$

The  $q \times q$  matrix  $\mathcal{H}_{\text{linkage}}^{(j)}$  in Eq. (4) can be regarded as a Hamiltonian of an isolated ‘‘molecule’’. In the present case, we assume that all the linkages have the same structure, i.e., the following holds:

$$\mathcal{H}_{\text{linkage}}^{(1)} = \mathcal{H}_{\text{linkage}}^{(2)} = \cdots = \mathcal{H}_{\text{linkage}}^{(D+1)} = \mathcal{H}_{\text{linkage}}. \quad (7)$$

## B. Derivation of flat-band solution

This type of models possess multiple flat bands with different energies [63, 68, 72]. Remarkably, if the number of decorated sites on each bond is  $q$ , there exist  $q$  flat bands with different energies. More precisely, in the  $D$ -dimensional model, each flat band has  $(D-1)$ -fold degeneracy, thus the number of flat bands is equal to  $(D-1)q$ .

In general, analytic solutions of the dispersion relations in this class of models are hard to obtain, since the size of the Hamiltonian matrix is large. Nevertheless, we can obtain the eigenvalues and eigenvectors of the flat bands as follows. Let  $\boldsymbol{\lambda}_{\text{linker},\mathbf{k}}$  be a  $(D+1)$ -component column vector, which satisfies

$$\Psi_{\mathbf{k}}^\dagger \boldsymbol{\lambda}_{\text{linker},\mathbf{k}} = \begin{pmatrix} 0 \\ 0 \end{pmatrix}. \quad (8)$$

As  $\Psi_{\mathbf{k}}^\dagger$  is the  $2 \times (D+1)$  matrix, there are  $D-1$  independent solutions of  $\boldsymbol{\lambda}_{\text{linker},\mathbf{k}}$ . Only at the  $\Gamma$  point (i.e.,

$\mathbf{k} = \mathbf{0}$ ), the rank of  $\Psi_{\mathbf{k}}^\dagger$  is reduced by one as  $\psi^{(1)} = \psi_{\mathbf{k}}^{(2)}$  holds, which results in the increase of the number of solutions from  $D-1$  to  $D$ . We note that  $\boldsymbol{\lambda}_{\text{linker},\mathbf{k}}$  corresponds to the flat-band eigenvector of the  $D$ -dimensional pyrochlore lattice [51].

To find the flat-band solution, we employ a notion of ‘‘intertwiner’’ [79, 80]. Before going to the concrete problem, we briefly address a generic argument. Let  $A$  and  $G$  be Hermitian matrices with different sizes. It is known that  $A$  and  $G$  have common eigenvalues if these matrices satisfy

$$AC = CG, \quad (9)$$

with  $C$  being a non-square matrix. The matrix  $C$  is called the ‘‘intertwiner’’. A simple proof of this statement is as follows. Let  $\phi$  be an eigenvector of  $G$  with eigenvalue  $\varepsilon$ . Then, one finds that  $C\phi$  is an eigenvector of  $A$  with eigenvalue  $\varepsilon$  (unless  $\phi$  belongs to the kernel of  $C$ ), because

$$A(C\phi) = CG\phi = \varepsilon(C\phi). \quad (10)$$

Turning to the present model, we can explicitly construct the intertwiner  $C_{\mathbf{k}}$  which is  $[(D+1)q+2] \times q$  matrix and satisfies

$$\mathcal{H}_{\mathbf{k}} C_{\mathbf{k}} = C_{\mathbf{k}} \mathcal{H}_{\text{linkage}}. \quad (11)$$

Its form is given as

$$C_{\mathbf{k}} = \begin{pmatrix} \mathbf{0}_q^T \\ [\boldsymbol{\lambda}_{\text{linker},\mathbf{k}}]_1 I_q \\ \vdots \\ [\boldsymbol{\lambda}_{\text{linker},\mathbf{k}}]_{D+1} I_q \\ \mathbf{0}_q^T \end{pmatrix}, \quad (12)$$

where  $\mathbf{0}_q$  stands for the  $q$ -component column zero vector,  $I_q$  stands for the  $q \times q$  identity matrix, and  $[\boldsymbol{\lambda}_{\text{linker},\mathbf{k}}]_j$  is the  $j$ -th component of  $\boldsymbol{\lambda}_{\text{linker},\mathbf{k}}$ . Therefore, the eigenvalues of  $\mathcal{H}_{\text{linkage}}$  are also those of  $\mathcal{H}_{\mathbf{k}}$ . As  $\mathcal{H}_{\text{linkage}}$  is  $\mathbf{k}$ -independent, the eigenvalues obtained as such naturally form flat bands. Equation (11) also leads to the flat-band wave function. Let  $\phi_{\text{linkage},n}$  be a  $q$ -component vector which is the  $n$ th eigenvector of  $\mathcal{H}_{\text{linkage}}$ . It satisfies

$$\mathcal{H}_{\text{linkage}} \phi_{\text{linkage},n} = \varepsilon_{\text{linkage},n} \phi_{\text{linkage},n} \quad (13)$$

with  $\varepsilon_{\text{linkage},n}$  being the eigenvalue. Then, the flat-band eigenvector  $\varphi_{\mathbf{k},n}$ , written as

$$\varphi_{\mathbf{k},n} = \begin{pmatrix} \varphi_{A,\mathbf{k},n} \\ \varphi_{1,\mathbf{k},n} \\ \vdots \\ \varphi_{(D+1)q,\mathbf{k},n} \\ \varphi_{B,\mathbf{k},n} \end{pmatrix}, \quad (14)$$

is given as

$$\varphi_{\mathbf{k},n} = \frac{1}{\mathcal{N}_{\mathbf{k}}} C_{\mathbf{k}} \phi_{\text{linkage},n}, \quad (15)$$

where  $\mathcal{N}_{\mathbf{k}}$  is the normalization constant. More concretely, the components of  $\varphi_{\mathbf{k},n}$  are given as

$$\varphi_{A,\mathbf{k},n} = \varphi_{B,\mathbf{k},n} = 0, \quad (16)$$

and

$$\varphi_{q(j-1)+m,\mathbf{k},n} = \frac{1}{\mathcal{N}_{\mathbf{k}}} [\lambda_{\text{linker},\mathbf{k}}]_j [\phi_{\text{linkage},n}]_m \quad (17)$$

with  $j = 1, \dots, D+1$  and  $m = 1, \dots, q$ . Equation (17) indicates that the flat-band wave function of the  $D$ -dimensional decorated diamond lattice is given by the product of the linkage's wave function and the flat-band wave function of  $D$ -dimensional pyrochlore lattice.

In the next section, we elucidate how this construction actually works by showing specific examples.

### III. EXAMPLES

In this section, we demonstrate that the aforementioned method works for decorated diamond lattices in  $D = 2, 3$  and 4. Although our formulation is applicable to generic types of decoration patterns, we mainly focus on the model where the chain-type structure is inserted between the neighboring sites of the diamond lattices. (We present an example of the non-chain-type decorating sites for  $D = 2$ ; see Fig. 4.) The motivation to focus on these models is that, for  $D = 2, 3$ , they are known to be relevant to MOFs such as DCBP<sub>3</sub>Co<sub>2</sub> and DCA<sub>3</sub>Co<sub>2</sub> [71],  $\alpha$ -graphyne [65–68], and TaS<sub>2</sub> [72, 73]. (DCBP and DCA stand for dicyanobiphenyl and dicyanoanthracene, respectively). As for  $D = 4$ , some recent works addressed the four-dimensional diamond lattice [81–83] as a canonical example of four-dimensional Dirac fermions on lattice models. In this context, the decorated four-dimensional diamond lattice is an interesting extension of it where Dirac fermions and flat bands coexist.

#### A. Two dimensions: Decorated honeycomb lattice

Consider a decorated honeycomb lattice model with  $q$  sites on each edge of hexagons [Fig. 3(a)]. The specific

form of the Hamiltonian,  $\mathcal{H}_{\mathbf{k}}^{\text{DH}}$ , is given by substituting  $t = t_1, t' = t_{q+1}$ , and

$$\mathcal{H}_{\text{linkage}}^{\text{DH}} = \begin{pmatrix} U_1 & t_2 & & & & \\ t_2 & U_2 & t_3 & & & \\ & & t_3 & U_3 & \ddots & \\ & & & \ddots & \ddots & \\ & & & & & U_{q-1} & t_q \\ & & & & & t_q & U_q \end{pmatrix} \quad (18)$$

into Eq. (4). The row vectors  $\psi^{\text{DH}(1)\dagger}$  and  $\psi_{\mathbf{k}}^{\text{DH}(2)\dagger}$  are given as

$$\psi^{\text{DH}(1)\dagger} = (1, 1, 1), \quad (19)$$

$$\psi_{\mathbf{k}}^{\text{DH}(2)\dagger} = (e^{-i\mathbf{k}\cdot\mathbf{a}_1^{\text{DH}}}, e^{-i\mathbf{k}\cdot\mathbf{a}_2^{\text{DH}}}, 1). \quad (20)$$

The vector  $\lambda_{\text{linker},\mathbf{k}}^{\text{DH}}$  is obtained as

$$\lambda_{\text{linker},\mathbf{k}}^{\text{DH}} = \begin{pmatrix} 1 - e^{-i\mathbf{k}\cdot\mathbf{a}_2^{\text{DH}}} \\ e^{-i\mathbf{k}\cdot\mathbf{a}_1^{\text{DH}}} - 1 \\ e^{-i\mathbf{k}\cdot\mathbf{a}_2^{\text{DH}}} - e^{-i\mathbf{k}\cdot\mathbf{a}_1^{\text{DH}}} \end{pmatrix}. \quad (21)$$

Then, the flat-band energies are equal to the eigenvalues of  $\mathcal{H}_{\text{linkage}}^{\text{DH}}$ , and the corresponding wave functions are given in the form of Eq. (17).

In Figs. 3(d)–(f), we plot the band structures for  $q = 3$  with several sets of parameters. In all cases, there are three flat bands, whose energies are indeed equal to  $\varepsilon_{\text{linkage},n}$ .

It is also interesting to find that the triple band touching, where the flat band penetrates the band touching point of dispersive bands, occurs at  $\Gamma$  point in some cases [e.g.,  $\varepsilon = 0$  in Fig. 3(d)]. In what follows, we elucidate the condition for the triple band touching, by explicitly derive the eigenenergies at  $\Gamma$  point.

Before proceeding further, we remark that any of the flat bands touches the dispersive band at  $\Gamma$  point regardless of the parameters. This is because of the rank reduction of  $\Psi_{\mathbf{k}}^{\dagger}$ , which we have mentioned in Sec. II A. Therefore, from the above derivation of the flat-band energies, we have already obtained  $2q$  eigenenergies out of  $3q + 2$  at  $\Gamma$  point, thus we need to derive the remaining  $q + 2$  eigenenergies.

For the derivation of the eigenenergies at  $\Gamma$  point, we first point out that the remaining eigenstates have three-fold rotational symmetries centered at A site and B site. Therefore, the wave function satisfies

$$\varphi_m = \varphi_{m+q} = \varphi_{m+2q}, \quad (22)$$

for  $m = 1, \dots, q$ . Substituting (22) into the Schrödinger equation, we find that it is reduced to the eigenvalue





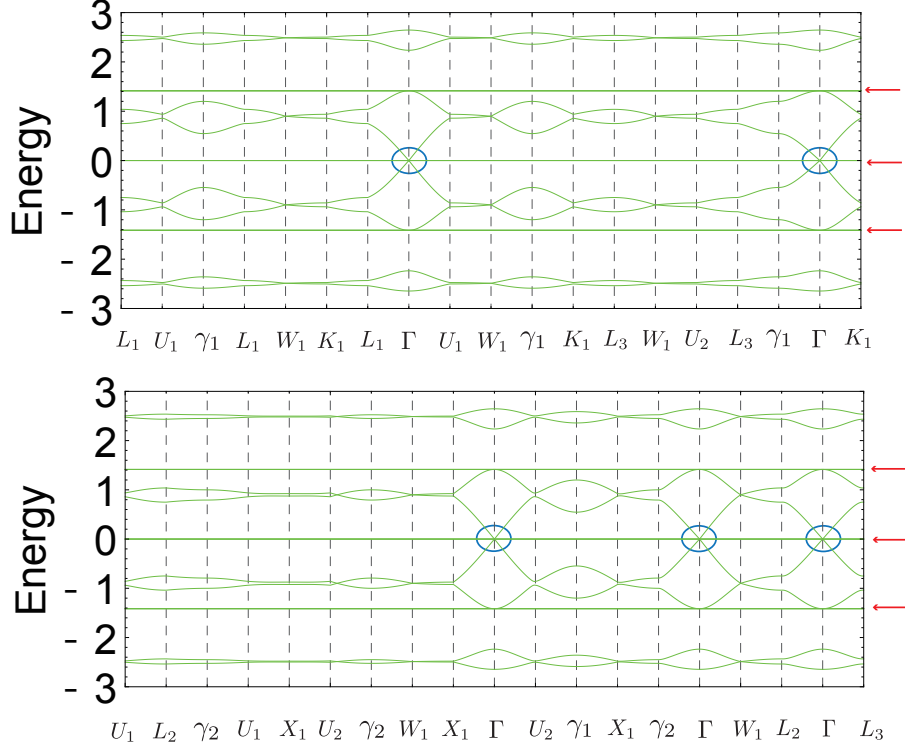


FIG. 7. The band structure of the decorated four-dimensional diamond lattice with  $q = 3$ . The parameters are set as  $(t_1, t_2, t_3, t_4, U_A, U_1, U_2, U_3, U_B) = (1, 1, 1, 1, 0, 0, 0, 0, 0)$ . Upper and lower panels are for different high-symmetry lines. Red arrows point to the flat bands, and blue circles represent the quintuple band touchings.

four-dimensional Brillouin zone, we follow Ref. [83]; see Appendix C. We note that the degeneracy of each flat band is two (three) for  $D = 3$  ( $D = 4$ ). Correspondingly, the band touchings at  $\Gamma$  point denoted by the blue circles in Figs. 6 and 7 have  $D + 1$ -fold degeneracy for the  $D$ -dimensional system.

#### IV. $D$ -DIMENSIONAL DECORATED PYROCHLORE LATTICES

In this section, we discuss yet another series of multiple flat-band systems, namely,  $D$ -dimensional decorated pyrochlore lattices. For concreteness, we consider the three-dimensional decorated pyrochlore model with one decorating site between neighboring tetrahedra [Fig. 8(a)]. Extension to generic dimensions and generic forms of decoration is straightforward. (For instance, the result for the two-dimensional analog is presented in the prior work [62].) We note that this type of lattice structure, both in two and three dimensions, has various material realizations, mainly in organic systems [60–62, 77, 86–88].

We consider the lattice of Fig. 8(a). Three lattice vectors are in common with the decorated diamond lattice.

The Hamiltonian is the  $12 \times 12$  matrix given as

$$\mathcal{H}_{\mathbf{k}}^{\text{DP}} = \begin{pmatrix} \tilde{\mathcal{H}}_{\text{linkage}}^{\text{DP}} & V_{\mathbf{k},(1,2)} & V_{\mathbf{k},(1,3)} & V_{\mathbf{k},(1,4)} \\ V_{\mathbf{k},(2,1)} & \tilde{\mathcal{H}}_{\text{linkage}}^{\text{DP}} & V_{\mathbf{k},(2,3)} & V_{\mathbf{k},(2,4)} \\ V_{\mathbf{k},(3,1)} & V_{\mathbf{k},(3,2)} & \tilde{\mathcal{H}}_{\text{linkage}}^{\text{DP}} & V_{\mathbf{k},(3,4)} \\ V_{\mathbf{k},(4,1)} & V_{\mathbf{k},(4,2)} & V_{\mathbf{k},(4,3)} & \tilde{\mathcal{H}}_{\text{linkage}}^{\text{DP}} \end{pmatrix}, \quad (28)$$

where

$$\tilde{\mathcal{H}}_{\text{linkage}}^{\text{DP}} = \begin{pmatrix} 0 & t_3 & 0 \\ t_3 & 0 & t_4 \\ 0 & t_4 & 0 \end{pmatrix}, \quad (29)$$

and

$$V_{\mathbf{k},(i,j)} = \begin{pmatrix} t_1 & 0 & 0 \\ 0 & 0 & 0 \\ 0 & 0 & t_2 e^{-i\mathbf{k} \cdot (\mathbf{a}_i^{\text{DD}} - \mathbf{a}_j^{\text{DD}})} \end{pmatrix} \quad (30)$$

with  $\mathbf{a}_4^{\text{DD}} = (0, 0, 0)$ .

To obtain the flat band solution, we again give the intertwiner explicitly. In the present model, we have

$$\mathcal{H}_{\mathbf{k}}^{\text{DP}} C_{\mathbf{k}} = C_{\mathbf{k}} \mathcal{H}_{\text{linkage}}^{\text{DP}}, \quad (31)$$

where

$$C_{\mathbf{k}} = \begin{pmatrix} [\lambda_{\text{linker},\mathbf{k}}]_1 I_3 \\ [\lambda_{\text{linker},\mathbf{k}}]_2 I_3 \\ [\lambda_{\text{linker},\mathbf{k}}]_3 I_3 \\ [\lambda_{\text{linker},\mathbf{k}}]_4 I_3 \end{pmatrix}, \quad (32)$$

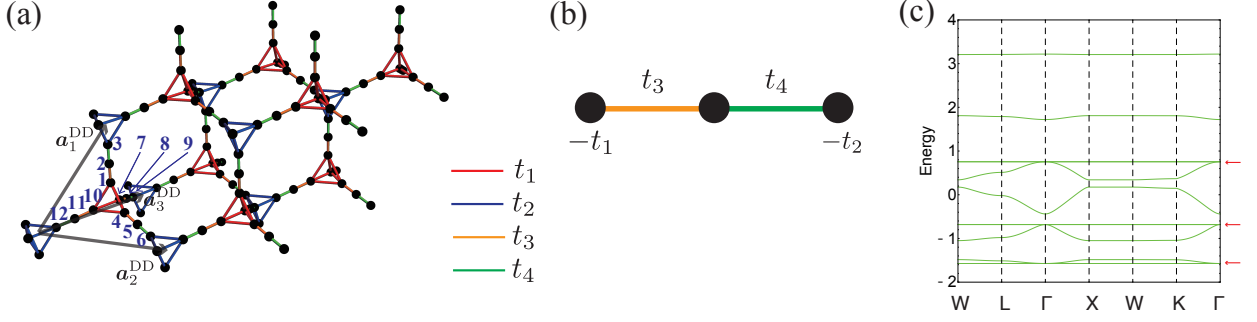


FIG. 8. (a) A decorated pyrochlore lattice with one decorated site between neighboring tetrahedra. (b) Schematic figure of the Hamiltonian of the chain-like molecule corresponding to  $\mathcal{H}_{\text{linkage}}^{\text{DP}}$ . (c) The band structure for  $(t_1, t_2, t_3, t_4) = (1, 0.5, 0.8, 0.7)$ . Red arrows point to the flat bands.

and

$$\begin{aligned} \mathcal{H}_{\text{linkage}}^{\text{DP}} &= \tilde{\mathcal{H}}_{\text{linkage}}^{\text{DP}} + \begin{pmatrix} -t_1 & 0 & 0 \\ 0 & 0 & 0 \\ 0 & 0 & -t_2 \end{pmatrix} \\ &= \begin{pmatrix} -t_1 & t_3 & 0 \\ t_3 & 0 & t_4 \\ 0 & t_4 & -t_2 \end{pmatrix}, \end{aligned} \quad (33)$$

where  $\lambda_{\text{linker}, \mathbf{k}}$  is the same as that for the decorated diamond model. Note that the left-hand side of Eq. (31) becomes

$$\begin{aligned} \mathcal{H}_{\mathbf{k}}^{\text{DP}} C_{\mathbf{k}} &= \begin{pmatrix} \tilde{\mathcal{H}}_{\text{linkage}}^{\text{DP}} & V_{\mathbf{k},(1,2)} & V_{\mathbf{k},(1,3)} & V_{\mathbf{k},(1,4)} \\ V_{\mathbf{k},(2,1)} & \tilde{\mathcal{H}}_{\text{linkage}}^{\text{DP}} & V_{\mathbf{k},(2,3)} & V_{\mathbf{k},(2,4)} \\ V_{\mathbf{k},(3,1)} & V_{\mathbf{k},(3,2)} & \tilde{\mathcal{H}}_{\text{linkage}}^{\text{DP}} & V_{\mathbf{k},(3,4)} \\ V_{\mathbf{k},(4,1)} & V_{\mathbf{k},(4,2)} & V_{\mathbf{k},(4,3)} & \tilde{\mathcal{H}}_{\text{linkage}}^{\text{DP}} \end{pmatrix} \begin{pmatrix} [\lambda_{\text{linker}, \mathbf{k}}]_1 I_3 \\ [\lambda_{\text{linker}, \mathbf{k}}]_2 I_3 \\ [\lambda_{\text{linker}, \mathbf{k}}]_3 I_3 \\ [\lambda_{\text{linker}, \mathbf{k}}]_4 I_3 \end{pmatrix} \\ &= \begin{pmatrix} [\lambda_{\text{linker}, \mathbf{k}}]_1 \tilde{\mathcal{H}}_{\text{linkage}}^{\text{DP}} + [\lambda_{\text{linker}, \mathbf{k}}]_2 V_{\mathbf{k},(1,2)} + [\lambda_{\text{linker}, \mathbf{k}}]_3 V_{\mathbf{k},(1,3)} + [\lambda_{\text{linker}, \mathbf{k}}]_4 V_{\mathbf{k},(1,4)} \\ [\lambda_{\text{linker}, \mathbf{k}}]_2 \tilde{\mathcal{H}}_{\text{linkage}}^{\text{DP}} + [\lambda_{\text{linker}, \mathbf{k}}]_1 V_{\mathbf{k},(2,1)} + [\lambda_{\text{linker}, \mathbf{k}}]_3 V_{\mathbf{k},(2,3)} + [\lambda_{\text{linker}, \mathbf{k}}]_4 V_{\mathbf{k},(2,4)} \\ [\lambda_{\text{linker}, \mathbf{k}}]_3 \tilde{\mathcal{H}}_{\text{linkage}}^{\text{DP}} + [\lambda_{\text{linker}, \mathbf{k}}]_1 V_{\mathbf{k},(3,1)} + [\lambda_{\text{linker}, \mathbf{k}}]_2 V_{\mathbf{k},(3,2)} + [\lambda_{\text{linker}, \mathbf{k}}]_4 V_{\mathbf{k},(3,4)} \\ [\lambda_{\text{linker}, \mathbf{k}}]_4 \tilde{\mathcal{H}}_{\text{linkage}}^{\text{DP}} + [\lambda_{\text{linker}, \mathbf{k}}]_1 V_{\mathbf{k},(4,1)} + [\lambda_{\text{linker}, \mathbf{k}}]_2 V_{\mathbf{k},(4,2)} + [\lambda_{\text{linker}, \mathbf{k}}]_3 V_{\mathbf{k},(4,3)} \end{pmatrix}. \end{aligned} \quad (34)$$

The  $j$ -th column of the second line of Eq. (34) is

$$\begin{aligned} &[\lambda_{\text{linker}, \mathbf{k}}]_j \tilde{\mathcal{H}}_{\text{linkage}}^{\text{DP}} + \sum_{j' \neq j} [\lambda_{\text{linker}, \mathbf{k}}]_{j'} \begin{pmatrix} t_1 & 0 & 0 \\ 0 & 0 & 0 \\ 0 & 0 & t_2 e^{-i\mathbf{k} \cdot (\mathbf{a}_j^{\text{DD}} - \mathbf{a}_{j'}^{\text{DD}})} \end{pmatrix} \\ &= [\lambda_{\text{linker}, \mathbf{k}}]_j \left[ \tilde{\mathcal{H}}_{\text{linkage}}^{\text{DP}} + \begin{pmatrix} -t_1 & 0 & 0 \\ 0 & 0 & 0 \\ 0 & 0 & -t_2 \end{pmatrix} \right] = [\lambda_{\text{linker}, \mathbf{k}}]_j \mathcal{H}_{\text{linkage}}^{\text{DP}}, \end{aligned} \quad (35)$$

which is equal to the  $j$ -th component of the right-hand side of Eq. (32). The second line of Eq. (35) can be obtained by using Eq. (8). Having Eq. (31) at hand, we again see that the flat-band eigenenergies are equal to those of  $\mathcal{H}_{\text{linkage}}^{\text{DP}}$ , and that the wave function of  $n$ th flat band is given as

$$\varphi_{3(j-1)+m, \mathbf{k}, n}^{\text{DP}} = \frac{1}{\mathcal{N}_{\mathbf{k}}} [\lambda_{\text{linker}, \mathbf{k}}]_j [\phi_{\text{linkage}, n}^{\text{DP}}]_m, \quad (36)$$

( $j = 1, 2, 3, 4$ ,  $m = 1, 2, 3$ ), where  $\phi_{\text{linkage}, n}^{\text{DP}}$  is the eigen-

vector of  $\mathcal{H}_{\text{linkage}}^{\text{DP}}$  corresponding to the  $n$ th eigenvalue. The corresponding molecule for  $\mathcal{H}_{\text{linkage}}^{\text{DP}}$  is depicted in Fig. 8(b). Comparing  $\tilde{\mathcal{H}}_{\text{linkage}}^{\text{DP}}$  with  $\mathcal{H}_{\text{linkage}}^{\text{DP}}$ , one finds that the on-site potentials,  $-t_1$  and  $-t_2$ , are added at the end sites.

The band structure for a certain set of parameters is shown in Fig. 8(c). We obtain three flat bands, each of which is doubly degenerate. As we have discussed, their energies are equal to the eigenvalues of  $\mathcal{H}_{\text{linkage}}^{\text{DP}}$ .



## V. SUMMARY AND DISCUSSIONS

We have presented the method to determine the flat-band energies and wave functions analytically in the decorated diamond lattices in arbitrary dimensions. The key idea is to divide the Hamiltonian into the linker part and the linkage part. Namely, by using the intertwiner [Eq. (11)] which is composed of the wave functions at the linker, we can reduce the eigenvalue problem of  $\mathbf{k}$ -dependent  $[(D+1)q+2] \times [(D+1)q+2]$  matrix ( $\mathcal{H}_{\mathbf{k}}$ ) to the  $\mathbf{k}$ -independent  $q \times q$  linkage Hamiltonian ( $\mathcal{H}_{\text{linkage}}$ ). Further, we also find that the flat-band wave function of the  $D$ -dimensional decorated diamond lattice is given by the product of the linkage wave function and the flat-band wave function for the  $D$ -dimensional pyrochlore lattice.

We show the examples of the decorated honeycomb lattice in two dimensions, the decorated diamond lattice in three dimensions, and the decorated four-dimensional diamond lattice, where each NN bond is decorated by the chain-like structure. The condition for the multiple band touching at  $\Gamma$  point is also addressed. Further, the same method is applicable to the  $D$ -dimensional decorated pyrochlore lattices. There, the tetrahedral parts of the original Hamiltonian turn into the on-site potential at the edges of the linkage Hamiltonian.

As mentioned in Sec. I, several extensions of our method are possible, as listed below.

- (i) We assume that each linkage is connected to a linker through one of the sites. However, this method can be used even when each linkage is connected to a linker with more than two sites [for an example, see Fig. 9(a)]. This is because the relation Eq. (11) for the intertwiner of Eq. (12) holds even in this case.
- (ii) We assume that all the hopping integrals in each linker are the same. This condition can be relaxed, i.e., the hopping integrals in each linker can be different [for an example, see Fig. 9(c)].
- (iii) We assume that all the linkages have the same structure [Eq. (7)]. However, our construction of the flat bands works even when linkages have different structures, as long as the linkages have common eigenenergies [76]. For instance, the numbers of sites consisting of the linkages can be different from each other [see Fig. 9(e)].
- (iv) Finally, the lattices structures are not limited to the decorated diamond lattices. In fact, the method works in, e.g., the decorated square lattices (i.e., the generalized Lieb lattices) [76]. In this regard, the Lieb-lattice-based materials are also in the scope of application of this method [89–91].

Although the comprehensive descriptions about the generalizations are beyond the scope of this paper, we show some of the results of the generalized models in Appendix A.

To conclude, there are a number of materials with decorated honeycomb, diamond and pyrochlore lattice structures, especially for organic materials. We hope that our method to determine flat-band energies and wave functions is useful for band structure analysis and material design.

*Note added.*— Recently, we became aware of the related works [92, 93] where the flat bands of the decorated honeycomb model are discussed.

## ACKNOWLEDGMENTS

This work is supported by JSPS KAKENHI, Grants No. JP17H06138 (T. M. and Y. H.) and No. JP20K14371 (T. M.). H. K. was supported in part by JSPS Grant-in-Aid for Scientific Research on Innovative Areas No. JP20H04630, JSPS KAKENHI Grant No. JP18K03445, and the Inamori Foundation.

### Appendix A: Examples of the extended models

In this appendix, we show two examples where the assumptions described in Sec. II are relaxed. Here we focus on the case of  $D = 2$ .

The first model is depicted in Fig. 9(a) (we set  $q = 4$ ), where two sites on each linkage are connected to a linker. Specifically, the second-neighbor hoppings  $t_6$  and  $t_7$  are included in addition to the NN hoppings. The band structure for a representative set of parameters is shown in Fig. 9(b). We see that there exist four exact flat bands. In fact, the flat-band energies and eigenvectors are given in exactly the same forms as described in the main text since Eq. (11) for the intertwiner of Eq. (12) holds even in this case. Therefore, the flat bands are not affected by the inclusion of the second-neighbor hoppings of this kind.

The second model is depicted in Fig. 9(c) (we set  $q = 3$ ), where the hopping integrals in each linker are different from each other. For instance, the linker including sublattice A contains three different hoppings,  $t_1$ ,  $t'_1$ , and  $t''_1$ . The band structure for a representative set of parameters is shown in Fig. 9(d). We see three exact flat bands. In fact, the flat bands can be obtained by replacing  $\lambda_{\text{linker},\mathbf{k}}$  in the intertwiner of Eq. (12) with  $\tilde{\lambda}_{\text{linker},\mathbf{k}}$ , which satisfies

$$\begin{pmatrix} t'_1 & t''_1 & t_1 \\ t'_4 e^{-i\mathbf{k} \cdot \mathbf{a}_1^{\text{DH}}} & t''_4 e^{-i\mathbf{k} \cdot \mathbf{a}_2^{\text{DH}}} & t_4 \end{pmatrix} \tilde{\lambda}_{\text{linker},\mathbf{k}} = \begin{pmatrix} 0 \\ 0 \end{pmatrix}. \quad (\text{A1})$$

The third model is depicted in Fig. 9(e), where the linkages are not the same. Specifically, two of three linkages around A have  $q = 2$  whereas the other has  $q = 1$ . Only for the linkage of  $q = 1$ , we introduce the on-site potential  $V$  so that all three linkages have a common eigenenergy. The band structure for a representative set of parameters is shown in Fig. 9(f). We see that there

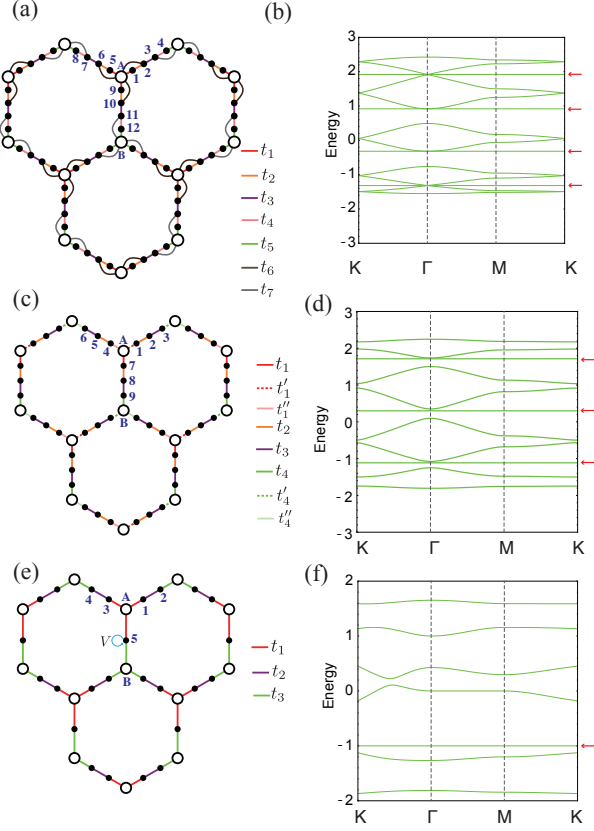


FIG. 9. The examples of the generalizations of the flat-band models on decorated honeycomb lattices. (a) Model where two sites on each linkage are connected to a linker. (b) Band structure for the model of (a). The parameters are set as  $(t_1, t_2, t_3, t_4, t_5, t_6, t_7, U_A, U_1, U_2, U_3, U_4, U_B) = (0.8, 1, 1, 1, 0.8, 0.2, 0.2, 0, 0.3, 0.3, 0.3, 0.3, 0)$  (The definitions of the above parameters follow those in Sec. III A). (c) Model where the hoppings integrals on each linker are different. (d) Band structure for the model of (c). The parameters are set as  $(t_1, t'_1, t''_1, t_2, t_3, t_4, t'_4, t''_4, U_A, U_1, U_2, U_3, U_B) = (0.8, 0.7, 0.6, 1, 1, 0.8, 0.9, 1, 0, 0.3, 0.3, 0.3, 0)$ . (e) Model where the linkages have the different structures from each other. (f) Band structure for the model of (e). The hopping parameters are set as  $(t_1, t_2, t_3) = (0.8, 1, 0.4)$ . The on-site potential is introduced only at the sublattice 5 with the energy  $V = -1$ . Red arrows point to the flat bands.

is an exact flat band, whose energy is the same as the common eigenenergy of the linkages.

### Appendix B: Specific cases with triple band touching

In this appendix, we elucidate that the condition for the triple band touching at  $\Gamma$  point in the decorated honeycomb model can be found exactly for the special case. Specifically, we restrict ourselves to the case where  $U_A = U_B = U_1 = \dots = U_q = 0$ ,  $t_2 = \dots = t_q = 1$ , and  $t_1 = t_{q+1} = \tilde{t}$ . The aim here is to determine  $\tilde{t}$  such that all of the  $q$  flat bands are involved in triple band touching

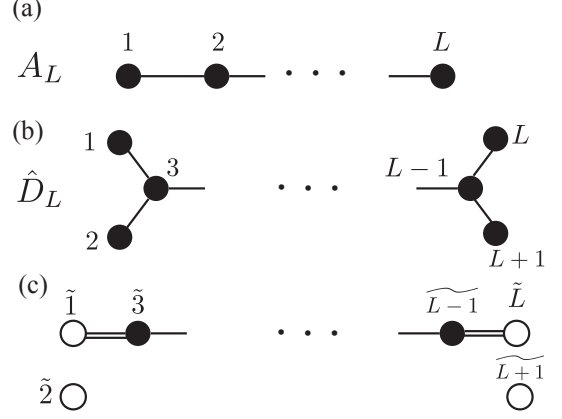


FIG. 10. The Dynkin diagram of (a)  $A_L$  and the extended Dynkin diagram of (b)  $\hat{D}_L$ . (c) Schematic figure of the chain plus two isolated sites equivalent to  $\hat{D}_L$  under the change of the basis. The single lines denote the bonds with the hopping being unity, while the double lines denote the bonds with the hopping being  $\sqrt{2}$ .

at  $\Gamma$  point, as shown in Fig. 3(f).

To this aim, we employ the wisdom of the eigenvalues of the adjacency matrices of the Dynkin diagrams (or A-D-E lattices). Specifically, for the present purpose, we consider the  $A$  type [Fig. 10(a)], which is nothing but the open chain, and the  $\hat{D}$  type [Fig. 10(b)], which has double branches at both ends. It is known [94, 95] that the eigenvalues of the adjacency matrix of  $A_L$  are given as

$$\varepsilon^{A_L} = 2 \cos \frac{j\pi}{L+1} \quad (j = 1, \dots, L), \quad (\text{B1})$$

while those of  $\hat{D}_L$  are given as

$$\varepsilon^{\hat{D}_L} = 0, 2 \cos \frac{j\pi}{L-2} \quad (j = 0, \dots, L-2). \quad (\text{B2})$$

From Eqs. (B1) and (B2), we see that all of the eigenvalues for  $A_L$  are included in the set of the eigenvalues of  $\hat{D}_{L+3}$ . We note that this fact can also be derived by explicitly giving the intertwiner between the adjacency matrices for these graphs. Namely, the following relation holds:

$$H_{\hat{D}_{L+3}} C_L = C_L H_{A_L}, \quad (\text{B3})$$

with

$$(C_L)_{ij} = \delta_{i,1} \delta_{j,1} + \delta_{i,j+1} - \delta_{i,j+3} - \delta_{i,L+4} \delta_{j,L} \quad (i = 1, \dots, L+4, j = 1, \dots, L), \quad (\text{B4})$$

where  $H_{\hat{D}_{L+3}}$  and  $H_{A_L}$  stand for the adjacency matrices of  $\hat{D}_{L+3}$  and  $A_L$ , respectively.

Further, as for  $\hat{D}_L$ , by changing the basis as  $|\tilde{1}\rangle = \frac{1}{\sqrt{2}}[|1\rangle + |2\rangle]$ ,  $|\tilde{2}\rangle = \frac{1}{\sqrt{2}}[|1\rangle - |2\rangle]$ ,  $|\tilde{L}\rangle = \frac{1}{\sqrt{2}}[|L\rangle + |L+1\rangle]$ ,  $|\tilde{L+1}\rangle = \frac{1}{\sqrt{2}}[|L\rangle - |L+1\rangle]$ , and

$|\tilde{\ell}\rangle = |\ell\rangle$  ( $\ell = 3, \dots, L-1$ ), where  $|\ell\rangle$  denotes the state localized at the  $\ell$ th site in the original graph, one can see that the hopping problem on the graph  $\hat{D}_L$  is equivalent to that on the  $(L-1)$ -site chain where the hoppings on the both of the ends are modulated from 1 to  $\sqrt{2}$  [see the double lines in Fig. 10(c)].

Combining these facts, we find the following: All of the eigenenergies of the  $q$ -site chain with the NN hopping being 1 are included in the set of the eigenenergies of the  $q+2$ -site chain where the hoppings are  $\sqrt{2}$  on the both of the ends and 1 otherwise. Turning to our original problem, we find that the multiple triple band touchings can be found by setting  $\sqrt{3\tilde{t}} = \sqrt{2}$ , which leads to  $\tilde{t} = \sqrt{\frac{2}{3}}$ . This is indeed the parameters employed for Fig. 3(f) (for  $q = 3$ ). It is to be stressed that the condition for  $\tilde{t}$  obtained here is regardless of  $q$ . In fact, for  $q = 2$ , the multiple triple band touchings were found in Ref. 68 for the same parameter choice. We also note that, for  $D$ -dimensional systems, the multiple band touchings whose degeneracy is  $D+1$  can be found for  $\tilde{t} = \sqrt{\frac{2}{D+1}}$ . An example of  $D = 3$  is shown in Fig. 6(d).

### Appendix C: High symmetry points of the first Brillouin zone in the four-dimensional diamond lattice

The four lattice vectors of the four-dimensional diamond lattice are

$$\mathbf{a}_1^{4\text{DD}} = \left( \frac{\sqrt{5}}{4}, \frac{\sqrt{5}}{4}, \frac{\sqrt{5}}{4}, \frac{5}{4} \right), \quad (\text{C1})$$

$$\mathbf{a}_2^{4\text{DD}} = \left( \frac{\sqrt{5}}{4}, -\frac{\sqrt{5}}{4}, -\frac{\sqrt{5}}{4}, \frac{5}{4} \right), \quad (\text{C2})$$

$$\mathbf{a}_3^{4\text{DD}} = \left( -\frac{\sqrt{5}}{4}, -\frac{\sqrt{5}}{4}, \frac{\sqrt{5}}{4}, \frac{5}{4} \right), \quad (\text{C3})$$

and

$$\mathbf{a}_4^{4\text{DD}} = \left( -\frac{\sqrt{5}}{4}, \frac{\sqrt{5}}{4}, -\frac{\sqrt{5}}{4}, \frac{5}{4} \right). \quad (\text{C4})$$

For the coordinates of the high-symmetry points in the first Brillouin zone in the four-dimensional diamond lattice, we follow Ref. 83:

$$\Gamma = (0, 0, 0, 0), \quad (\text{C5})$$

$$\gamma_1 = \left( 0, 0, 0, -\frac{4\pi}{5} \right), \quad (\text{C6})$$

$$\gamma_2 = \left( \frac{2\pi}{\sqrt{5}}, 0, 0, -\frac{2\pi}{5} \right), \quad (\text{C7})$$

$$L_1 = \left( \frac{4\pi}{5\sqrt{5}}, -\frac{4\pi}{5\sqrt{5}}, \frac{4\pi}{5\sqrt{5}}, -\frac{4\pi}{5} \right), \quad (\text{C8})$$

$$L_2 = \left( \frac{2\pi}{\sqrt{5}}, -\frac{2\pi}{5\sqrt{5}}, \frac{2\pi}{5\sqrt{5}}, -\frac{2\pi}{5} \right), \quad (\text{C9})$$

$$L_3 = \left( \frac{4\pi}{5\sqrt{5}}, \frac{4\pi}{5\sqrt{5}}, \frac{4\pi}{5\sqrt{5}}, -\frac{4\pi}{5} \right), \quad (\text{C10})$$

$$W_1 = \left( \frac{8\pi}{5\sqrt{5}}, 0, \frac{4\pi}{5\sqrt{5}}, -\frac{4\pi}{5} \right), \quad (\text{C11})$$

$$K_1 = \left( \frac{6\pi}{5\sqrt{5}}, 0, \frac{6\pi}{5\sqrt{5}}, -\frac{4\pi}{5} \right), \quad (\text{C12})$$

$$X_1 = \left( \frac{8\pi}{5\sqrt{5}}, 0, 0, -\frac{4\pi}{5} \right), \quad (\text{C13})$$

$$U_1 = \left( \frac{8\pi}{5\sqrt{5}}, -\frac{2\pi}{5\sqrt{5}}, \frac{2\pi}{5\sqrt{5}}, -\frac{4\pi}{5} \right), \quad (\text{C14})$$

$$U_2 = \left( \frac{8\pi}{5\sqrt{5}}, \frac{2\pi}{5\sqrt{5}}, \frac{2\pi}{5\sqrt{5}}, -\frac{4\pi}{5} \right). \quad (\text{C15})$$

- 
- [1] O. Vafek and A. Vishwanath, *Annu. Rev. Condens. Matter Phys.* **5**, 83 (2014).  
[2] N. P. Armitage, E. J. Mele, and A. Vishwanath, *Rev. Mod. Phys.* **90**, 015001 (2018).  
[3] A. Bernevig, H. Weng, Z. Fang, and X. Dai, *J. Phys. Soc. Jpn.* **87**, 041001 (2018).  
[4] K. S. Novoselov, E. McCann, S. V. Morozov, V. I. Fal'ko, M. I. Katsnelson, U. Zeitler, D. Jiang, F. Schedin, and A. K. Geim, *Nat. Phys.* **2**, 177 (2006).  
[5] K. Fukushima, D. E. Kharzeev, and H. J. Warringa, *Phys. Rev. D* **78**, 074033 (2008).  
[6] A. A. Zyuzin, S. Wu, and A. A. Burkov, *Phys. Rev. B* **85**, 165110 (2012).  
[7] H. Fukuyama and R. Kubo, *J. Phys. Soc. Jpn.* **28**, 570 (1970).  
[8] M. Koshino and T. Ando, *Phys. Rev. B* **76**, 085425 (2007); *Phys. Rev. B* **81**, 195431 (2010).  
[9] A. Raoux, F. Piéchon, J.-N. Fuchs, and G. Montambaux, *Phys. Rev. B* **91**, 085120 (2015).  
[10] H. Maebashi, M. Ogata, and H. Fukuyama, *J. Phys. Soc. Jpn.* **86**, 083702 (2017).  
[11] J. V. von Neumann and E. Wigner, *Physik Z.* **30**, 467 (1929).  
[12] Y. Hatsugai, *N. J. Phys.* **12**, 065004 (2010).  
[13] K. Asano and C. Hotta, *Phys. Rev. B* **83**, 245125 (2011).  
[14] A. Mielke, *J. Phys. A: Math. Gen.* **24** L73 (1991); *J. Phys. A: Math. Gen.* **24** 3311 (1991).  
[15] H. Tasaki, *Phys. Rev. Lett.* **69**, 1608 (1992).  
[16] A. Mielke and H. Tasaki, *Commun. Math. Phys.* **158**, 341 (1993).  
[17] K. Kusakabe and H. Aoki, *Phys. Rev. Lett.* **72**, 144 (1994).  
[18] H. Tasaki, *Prog. Theor. Phys.* **99**, 489 (1998).  
[19] K. Tamura and H. Katsura, *Phys. Rev. B* **100**, 214423 (2019).  
[20] H. Tasaki, *Physics and Mathematics of Quantum Many-Body Systems*, Springer, Berlin (2020).  
[21] M. Imada and M. Kohno, *Phys. Rev. Lett.* **84**, 143

- (2000).
- [22] K. Kuroki, T. Higashida, R. Arita, Phys. Rev. B **72**, 212509 (2005).
- [23] K. Kobayashi, M. Okumura, S. Yamada, M. Machida, and H. Aoki, Phys. Rev. B **94**, 214501 (2016).
- [24] K. Matsumoto, D. Ogura, and K. Kuroki, Phys. Rev. B **97**, 014516 (2018).
- [25] H. Aoki, Journal of Superconductivity and Novel Magnetism **33**, 2341 (2020).
- [26] H. Aoki, M. Ando, and H. Matsumura, Phys. Rev. B **54**, R17296(R) (1996).
- [27] J. Vidal, R. Mosseri, and B. Douçot, Phys. Rev. Lett. **81**, 5888 (1998).
- [28] H. M. Guo and M. Franz, Phys. Rev. B **80**, 113102 (2009).
- [29] C. Weeks and M. Franz, Phys. Rev. B **82**, 085310 (2010).
- [30] H. Katsura, I. Maruyama, A. Tanaka, and H. Tasaki, Europhys. Lett. **91** 57007 (2010).
- [31] D. Green, L. Santos, and C. Chamon, Phys. Rev. B **82**, 075104 (2010).
- [32] E. Tang, J.-W. Mei, and X.-G. Wen, Phys. Rev. Lett. **106**, 236802 (2011).
- [33] K. Sun, Z. Gu, H. Katsura, and S. Das Sarma, Phys. Rev. Lett. **106** 236803 (2011).
- [34] T. Neupert, L. Santos, C. Chamon, and C. Mudry, Phys. Rev. Lett. **106**, 236804 (2011).
- [35] D. N. Sheng, Z.-C. Gu, K. Sun, and L. Sheng, Nat. Commun. **2**, 389 (2011).
- [36] F. Wang and Y. Ran, Phys. Rev. B **84**, 241103(R) (2011).
- [37] Z. Liu, E. J. Bergholtz, H. Fan, and A. M. Läuchli, Phys. Rev. Lett. **109**, 186805 (2012).
- [38] B. Pal, Phys. Rev. B **98**, 245116 (2018).
- [39] J. W. Rhim and B.-J. Yang, Phys. Rev. B **99**, 045107 (2019).
- [40] T. Mizoguchi and Y. Hatsugai, Phys. Rev. B **101**, 235125 (2020).
- [41] Y. Kuno, Phys. Rev. B **101**, 184112 (2020).
- [42] Y. Kuno, T. Mizoguchi, and Y. Hatsugai, Phys. Rev. A **102**, 063325 (2020).
- [43] M. Goda, S. Nishino, and H. Matsuda, Phys. Rev. Lett. **96**, 126401 (2006).
- [44] J. T. Chalker, T. S. Pickles, and P. Shukla, Phys. Rev. B **82**, 104209 (2010).
- [45] T. Bilitewski and R. Moessner, Phys. Rev. B **98**, 235109 (2018).
- [46] Y. Kuno, T. Orito, and I. Ichinose, N. J. Phys. **22**, 013032 (2020).
- [47] C. Danieli, A. Andreanov, and S. Flach, Phys. Rev. B **102**, 041116(R) (2020).
- [48] T. Orito, Y. Kuno, and I. Ichinose, Phys. Rev. B **103**, L060301 (2021).
- [49] B. Sutherland, Phys. Rev. B **34**, 5208 (1986).
- [50] S. Miyahara, K. Kubo, H. Ono, Y. Shimomura, and N. Furukawa, J. Phys. Soc. Jpn. **74**, 1918 (2005).
- [51] Y. Hatsugai and I. Maruyama, Europhys. Lett. **95**, 20003 (2011).
- [52] W. Maimaiti, A. Andreanov, H. C. Park, O. Gendelman, and S. Flach, Phys. Rev. B **95**, 115135 (2017).
- [53] T. Misumi and H. Aoki, Phys. Rev. B **96**, 155137 (2017).
- [54] W. Maimaiti, S. Flach, and A. Andreanov, Phys. Rev. B **99**, 125129 (2019).
- [55] T. Mizoguchi and M. Udagawa, Phys. Rev. B **99**, 235118 (2019).
- [56] T. Mizoguchi and Y. Hatsugai, Europhys. Lett. **127**, 47001 (2019).
- [57] C.-C. Lee, A. Fleurence, Y. Yamada-Takamura, and T. Ozaki, Phys. Rev. B **100**, 045150 (2019).
- [58] W. Maimaiti, A. Andreanov, and S. Flach, Phys. Rev. B **103**, 165116 (2021).
- [59] Y. Hatsugai, K. Shiraiishi, and H. Aoki, N. J. Phys. **17**, 025009 (2015).
- [60] Y. Fujii, M. Maruyama, and S. Okada, Jpn. J. Appl. Phys. **57**, 125203 (2018).
- [61] Y. Fujii, M. Maruyama, and S. Okada, Jpn. J. Appl. Phys. **58**, 085001 (2019).
- [62] T. Mizoguchi, M. Maruyama, S. Okada, and Y. Hatsugai, Phys. Rev. Mater. **3**, 114201 (2019).
- [63] N. Shima and H. Aoki, Phys. Rev. Lett. **71**, 4389 (1993).
- [64] N. Morishita and K. Kusakabe, arXiv:2102.03835.
- [65] R. H. Baughman, H. Eckhardt, and M. Kertesz, J. Chem. Phys. **87**, 6687 (1987).
- [66] R. Longuinhos, E. A. Moujaes, S. S. Alexandre, and R. W. Nunes, Chem. Mater. **26**, 3701 (2014).
- [67] Z. Li, M. Smeu, A. Rives, V. Maraval, R. Chauvin, M. A. Ratner, and E. Borguet, Nat. Commun. **6**, 6321 (2015).
- [68] C. Barreteau, F. Ducastelle, and T. Mallah, J. Phys.: Condens. Matter **29**, 465302 (2017).
- [69] Z. Liu, Z.-F. Wang, J.-W. Mei, Y.-S. Wu, and F. Liu, Phys. Rev. Lett. **110**, 106804 (2013).
- [70] M. G. Yamada, T. Soejima, N. Tsuji, D. Hirai, M. Dincă, and H. Aoki, Phys. Rev. B **94**, 081102(R) (2016).
- [71] A. Kumar, K. Banerjee, A. S. Foster, and P. Liljeroth, Nano Lett. **18**, 5596 (2018).
- [72] J. M. Lee, C. Geng, J. W. Park, M. Oshikawa, S.-S. Lee, H. W. Yeom, and G. Y. Cho, Phys. Rev. Lett. **124**, 137002 (2020).
- [73] J. W. Park, G. Y. Cho, J. Lee, and H. W. Yeom, Nat. Commun. **10**, 4038 (2019).
- [74] T. Mizoguchi, Y. Kuno, and Y. Hatsugai, Phys. Rev. A **102**, 033527 (2020).
- [75] T. Mizoguchi, T. Yoshida, and Y. Hatsugai, Phys. Rev. B **103**, 045136 (2021).
- [76] H. Katsura and I. Maruyama, Kotai Butsuri **50**, 257-269 (2015) (in Japanese).
- [77] J.-Y. You, B. Gu, and G. Su, Sci. Rep. **9**, 20116 (2019).
- [78] Note that  $\Psi_{\mathbf{k}}^{\dagger}$  was called the “molecular orbital” (MO) for the  $D$ -dimensional pyrochlore model [51], by which the Hamiltonian of the tight-binding model with NN hoppings being  $t$  can be written as  $\mathcal{H}_{\mathbf{k}}^{\text{Py}} = t [\Psi_{\mathbf{k}} \Psi_{\mathbf{k}}^{\dagger} - 2I_{D+1}]$ , with  $I_{D+1}$  being the  $(D+1) \times (D+1)$  identity matrix.
- [79] P. Di Francesco and J.-B. Zuber, Nucl. Phys. B **338**, 602 (1990).
- [80] P. A. Pearce and Y.-K. Zhou, Int. J. Mod. Phys. B **7**, 3649 (1993).
- [81] M. Creutz, JHEP **04**, 017 (2008).
- [82] T. Kimura and T. Misumi, Prog. Theor. Phys. **123**, 63 (2010); *ibid.* **124**, 415 (2010).
- [83] Y. Kato and M. Yamanaka, J. Phys. Soc. Jpn. **86**, 033601 (2017).
- [84] F. D. M. Haldane, Phys. Rev. Lett. **61**, 2015 (1988).
- [85] T. Fukui, Y. Hatsugai, and H. Suzuki, J. Phys. Soc. Jpn. **74**, 1674 (2005).
- [86] X.-L. Sheng, Q.-B. Yan, F. Ye, Q.-R. Zheng, and G. Su, Phys. Rev. Lett. **106**, 155703 (2011).
- [87] C. Janani, J. Merino, I. P. McCulloch, and B. J. Powell, Phys. Rev. Lett. **113**, 267204 (2014).

- [88] C. Peng, Y. Xie, Z. Zhang, and Y. Chen, *International Journal of Heat and Mass Transfer* **164**, 120483 (2021).
- [89] B. Cui, X. Zheng, J. Wang, D. Lui, S. Xie, and B. Huang, *Nat. Commun.* **11**, 66 (2020).
- [90] X. Mao, J. Liu, J. Zhong, and R. A. Römer, *Physica E* **124**, 114340 (2020).
- [91] J. Liu, X. Mao, J. Zhong, and R. A. Römer, arXiv:2102.00161.
- [92] Z. Qi, E. Bobrow, and Y. Li, arXiv:2012.07806.
- [93] N. Boudjada, F. L. Buessen, and A. Paramekanti, *Phys. Rev. B* **103**, 165408 (2021).
- [94] A. E. Brouwer and W. H. Haemers, *Spectra of Graphs*, Springer, New York (2012).
- [95] M. Henkel, *Conformal Invariance and Critical Phenomena*, Springer, Berlin Heidelberg (1999).